J. Min. Metall. Sect. B-Metall. 55 (3) B (2019) 427 - 437

Journal of Mining and Metallurgy, Section B: Metallurgy

AB INITIO AND CALPHAD-TYPE THERMODYNAMIC INVESTIGATION OF THE Ti–Al–Zr SYSTEM

Z.-X. Deng [a,b], D.-P. Zhao [a,*], Y.-Y. Huang [b], L.-L. Chen [b], H. Zou [b], Y. Jiang [b], K. Chang [b,*]

[a*]College of Biology, Hunan University, Changsha, Hunan, China
[b] Key Laboratory of Marine Materials and Related Technologies, Zhejiang Key Laboratory of Marine Materials and Protective Technologies, Ningbo Institute of Materials Technology and Engineering, Chinese Academy of Sciences, Ningbo, China

(Received 22 October 2018; accepted 05 September 2019)

Abstract

Ti–Al based alloys have been widely used in the aeronautics and aerospace. Adding alloying element Zr can significantly improve their high-temperature endurance and corrosion resistance. To investigate the influence of the addition of element Zr on the properties of the Ti–Al system, ab initio calculations and the CALPHAD (CALculation of PHAse Diagrams) method were used to evaluate the Ti–Al–Zr ternary system. Ab initio calculations were carried out to calculate the formation enthalpies of intermetallic compounds and end-members. CALPHAD approach was employed to optimize the thermodynamic parameters based on experiments. The experimental data of phase equilibria at 1073, 1273, 1473, and 1573 K, as well as a vertical section of the Ti_3Al–Ti + 5 wt.% Zr were used to assess this system. The thermodynamic parameters of the binary Ti–Al, Al–Zr and Ti–Zr systems were acquired from recent assessments, and the ternary ones were evaluated in the present work. The Ti–Al–Zr ternary dataset has been established and the calculated results are in close agreement with the experimental data on both thermodynamics and phase equilibria.

Keywords*: Ti–Al–Zr system; Ab initio calculations; Phase diagrams; Thermodynamic optimization*

1. Introduction

Ti–Al based alloys are widely applied in the aeronautics and aerospace, owing to their good high-temperature strength and outstanding oxidation resistance, low density, and low thermal [1-4]. However, the poor room temperature ductility and fracture toughness of Ti−Al alloys significantly limit their applications [5-7]. The addition of elements has been used to improve the mechanical performance of alloy materials for a long time [8-11]. Recently Hashimoto [12] found that the addition of Zr increases the high-temperature endurance and superior corrosion resistance for the Ti–Al base alloys. Furthermore, the addition of Zr also improves ductility and toughness, and thus enhances the processability of Ti−Al base alloys at room temperature [13-15]. The experimental results indicated that Zr could stabilize the highly symmetric cubic $ZrAl_3$_$L1_2$ crystal structure which improves ductility and toughness against the low symmetric tetragonal $TiAl_3$_$D0_{22}$ structure [15]. The $ZrAl_3$ phase may serve as potential nucleation core for α(Al), thus resulting in a homogeneous microstructure with improved machinability of the related Ti–Al alloys [16].

The knowledge of thermodynamics and phase diagrams are constructive in material design, research, and development, especially for the development of the complex alloys [17]. Therefore, the information about phase diagrams of the Ti–Al–Zr system is significant for the design and fabrication of Ti–Al–Zr alloys. So far , there are only a few thermodynamic data and phase diagram data about Ti–Al–Zr system. *Ab initio* calculations is an effective method to obtain reliable thermodynamic data [18, 19]. The limited experimental data combined with *ab initio* calculations results are more effective for optimization. After the Ti–Al–Zr dataset is obtained, it can be used as a guidance for the experimental work to significantly reduce costs and resources. Hence, a thermodynamic assessment of the ternary Ti–Al–Zr system is necessary.

2. Literature review

2.1 Ti–Al

There are seven intermetallic compounds in this binary sytem, i.e., $Ti_3Al(\alpha_2)$, $TiAl(\gamma)$, Ti_3Al_5, $TiAl_2(\eta)$, $Ti_2Al_5(\zeta)$, $TiAl_3$(h) and $TiAl_3$(l). Their crystallographic

**Corresponding author: dpzhao@hnu.edu.cn; changkeke@nimte.ac.cn*

https://doi.org/10.2298/JMMB181022039D

data are summarized in Table 1. 'h' represents the high-temperature phase and 'l' represents the low-temperature phase for $TiAl_3$ phase. Their Pearson symbol and lattice parameters are different. The researchers [20, 21] assessed the experimental results [22-24], calculated phase diagrams [25-27], and proposed a quite similar phase diagram. Most recently, Witusiewicz et al. [28] reported a thermodynamic description of the Ti–Al system which can reproduce the majority of experimental data on phase equilibria and thermodynamic properties. Therefore, the thermodynamic functions assessed by Witusiewicz et al. [28] were accepted in the present work. The Ti–Al binary phase diagram is shown in Fig. 1 (a).

2.2 Al–Zr

There are ten intermetallic compounds in this binary sytsem, i.e., Zr_3Al, Zr_2Al, Zr_5Al_3, Zr_3Al_2, Zr_4Al_3, Zr_5Al_4, ZrAl, Zr_2Al_3, $ZrAl_2$ and $ZrAl_3$. Their crystallographic data are summarized in Table 1. The phase equilibria data before 1992 were reviewed and summarized by Murray [29] and then revised by Okamoto [30] to include the new results of Peruzzi [31]. Batalin et al. [32] determined the activity of Al in Al-rich liquid alloys at 1123 K. Klein et al. [33] determined the standard enthalpy of formation for the $ZrAl_2$ phase from the calorimetric measurement. Meschel and Kleppa [34] measured the standard enthalpies of $ZrAl_2$ and $ZrAl_3$ again by direct synthesis calorimetry at 1473 K. Esin et al. [35] measured the enthalpies of Zr_2Al_3, $ZrAl_2$, and $ZrAl_3$ in the temperature range 300 to 2000 K. Wang et al. [36] optimized the Al–Zr binary system combined with previous work, and the results are in good agreement with the experimental data [31, 37, 38]. Therefore, the optimized parameters done by Wang et al. [36] are adopted. The Al–Zr binary phase diagram is shown in Fig. 1 (b).

2.3 Ti–Zr

There are no intermetallic compounds in this binary system. The phase relationships of the Ti–Zr system are relatively simple. There are only three stable solution phases in this system, i.e., the liquid, bcc, and hcp phase. It is characterized by two congruent transformations: liquid to bcc, and bcc to hcp, The system was critically evaluated by Murray [44, 45], and then it was optimized based on the available experimental data [46, 47] by Hari Kumar et al. [48]. The results show a good agreement with experimental data [46, 47]. The thermodynamic description of the Ti–Zr system reported by Hari Kumar et al. [48] is chosen in the present work. The Ti–Zr binary phase diagram is shown in Fig. 1 (c).

2.4 Ti–Al–Zr

Shirokova et al. [49] determined the Ti_3Al–Ti + 5 wt.% Zr vertical section of the Ti–Al–Zr system with Equilibrated Alloys (EA) and Microanalysis (MA) methods. Numerous samples with different compositions were prepared and annealed at 1073 K for 1100 hours. The microstructure of each alloy was obtained by MA, followed by the Thermal Analysis (TA) to determine the phase boundary of a, $a_2(Ti_3Al)$, b, and liquid phases. Kainuma et al. [50] measured the phase equilibria in the Ti-rich corner of the Ti–Al–Zr system at 1273, 1473, and 1573 K by Electron Probe Micro Analysis (EPMA). Yang et al. [51] investigated the phase equilibria at 1273 K through alloy sampling combined with EPMA and XRD. The BSE images and XRD results intuitively reflected the phase regions. The composition of each phase was obtained by EPMA (Standard deviations of the measured concentration is ± 0.6 at.%), and thus the phase boundary was determined. The works of Yang et al. [51] were assessed to be more reliable than others [52, 53] due to the intuitive and accurate experimental results, higher emphasis would be placed on these data [51] in the present optimization. More recently, Lü et al. [52] determined the phase relationships at 1073 K (temperature error is within ± 5 °C) using equilibrated alloys and diffusion couple approach. They declared that there were two three-phase regions of TiAl + Ti_3Al + b(Ti, Zr) and TiAl + $ZrAl_2$ + b(Ti, Zr) in the diffusion couple. However, there were no obvious contrasts in the BSE images and no XRD patterns were presented for equilibrated alloys or diffusion couples. The two three-phase regions [52] remained uncertain and thus were not considered in the present work. Instead, we used other phase equilibria data [52] with solid evidences in the optimization. Ghosh et al. [53] calculated the enthalpies of formation along the $TiAl_3$–$ZrAl_3$ section. They only calculated five different points and there was no experimental data to support their results [53]. Therefore, we did not accept their data [53] in the present work. According to the reported data [50-53], no ternary compound exist in the ternary system. Table 2 summarizes the experimental data of the Ti-Al-Zr system accepted in the present optimization.

3. Methods and models

3.1 Ab initio calculations

The *ab initio* calculations based on density functional theory were carried out using the Vienna *ab initio* simulation package (VASP) [55], wherein projector augmented plane-wave potentials were employed [56]. The generalized gradient approximation (GGA) method was performed with the Blöchl corrections for the total energy [57]. A

Table 1. *List of symbols and crystallographic data of the phases in the Ti–Al–Zr system*

Phase	Space Group	Pearson symbol	Proto–type	Lattice parameters (Å)			References
				a	b	c	
α(Al)	$Fm\bar{3}m$	cF4	Cu	4.049	4.049	4.049	Al-5 vol.% Al3Zr [39]
α(Ti)	*P63/mmc*	hP2	Mg	2.95	2.95	4.684	Pure αTi [40]
α(Zr)	*P63/mmc*	hP2	Mg	3.232	3.232	5.148	Pure αZr [40]
β(Ti)	$Im\bar{3}m$	cI2	W	3.307	3.307	3.307	Pure βTi [41]
β(Zr)	$Im\bar{3}m$	cI2	W	3.609	3.609	3.609	Pure βZr [41]
Ti_3Al(α2)	*P63/mmc*	hP8	Ni3Sn	5.806	5.806	4.655	[42]
				5.739	5.739	4.645	This work (cal.)
TiAl(γ)	*P4/mmm*	tP4	CuAu	2.829	2.829	4.071	[24]
				2.829	2.829	4.071	This work (cal.)
Ti_3Al_5	*P4/mbm*	tP32	Ti_3Al_5	11.293	11.293	4.038	[28]
				–	–	–	–
$TiAl_2$(η)	*I41/amd*	tI24	$HfGa_2$	3.97	3.97	24.309	[24]
				3.967	3.967	24.273	This work (cal.)
Ti_2Al_5(ζ)	*P4/mmm*	tP28	Ti_2Al_5	3.905	3.905	29.196	[24]
				–	–	–	–
$TiAl_3$(h)	*I4/mmm*	tI8	$TiAl_3$(h)	3.863	3.863	8.648	[43]
				3.85	3.85	8.625	This work (cal.)
$TiAl_3$(l)	*I4/mmm*	tI32	$TiAl_3$(l)	3.987	3.875	33.84	[43]
				–	–	–	–
Zr_3Al	$Pm\bar{3}m$	cP4	Cu_3Au	4.373	4.373	4.373	[21]
				4.382	4.382	4.382	This work (cal.)
Zr_2Al	*P63/mmc*	hP6	Ni_2In	4.882	4.882	5.918	[29]
				4.906	4.906	5.934	This work (cal.)
Zr_5Al_3	*I4/mcm*	tI32	W_5Si_3	11.042	11.042	5.393	[29]
				11.078	11.078	5.386	This work (cal.)
Zr_3Al_2	*P42/mnm*	tP20	Zr_3Al_2	7.632	7.632	6.997	[29]
				7.675	7.675	6.963	This work (cal.)
Zr_4Al_3	*P6/mmm*	hP7	Zr_4Al_3	5.43	5.43	5.39	[29]
				5.444	5.444	5.408	This work (cal.)
Zr_5Al_4	*P63/mcm*	hP18	Ga_4Ti_5	8.447	8.447	5.785	[29]
				8.463	8.463	5.795	This work (cal.)
ZrAl	*Cmcm*	oC8	CrB	3.36	10.89	4.27	[29]
				3.352	10.946	4.302	This work (cal.)
Zr_2Al_3	*Fdd2*	oF40	Zr_2Al_3	9.601	13.91	5.578	[29]
				9.631	13.955	5.59	This work (cal.)
$ZrAl_2$	*P63/mmc*	hP12	$MgZn_2$	5.28	5.28	8.748	[29]
				5.291	5.291	8.789	This work (cal.)
$ZrAl_3$	*I4/mmm*	tI16	$ZrAl_3$	4.01	4.01	17.3	[29]
				4.018	4.018	17.336	This work (cal.)

plane-wave cutoff energy of 550 eV and an energy convergence criterion of 0.01 meV for electronic structure self-consistency were used. The integration in the Brillouin zone was performed on appropriate *k*-points, which was determined according to the Monkhorst-Pack method [58]. All structures are relaxed with respect to atomic positions and volumes. In the present work, the formation enthalpy, $\Delta H_f(Me_xAl_y$, Me=Ti or Zr) at 0 K is expressed by the following equation:

$$\Delta H_f(Me_xAl_y) = E(Me_xAl_y) - [x_{Me}E(Me) + x_{Al}E(Al)] \quad (1)$$

Where $E(Me_xAl_y)$, denote the total energy of Me_xAl_y . E(Me) and E(Al) are the energies of pure element for particular reference state. x_{Me} (Me = Ti or Zr) is the atomic fraction of the component.

3.2 CALPHAD

The CALPHAD-type modeling was performed with the step-by-step optimization procedure described by Du et al. [59]. The reliable experimental data and the enthalpies of formation for the compounds *via ab initio* calculations were employed

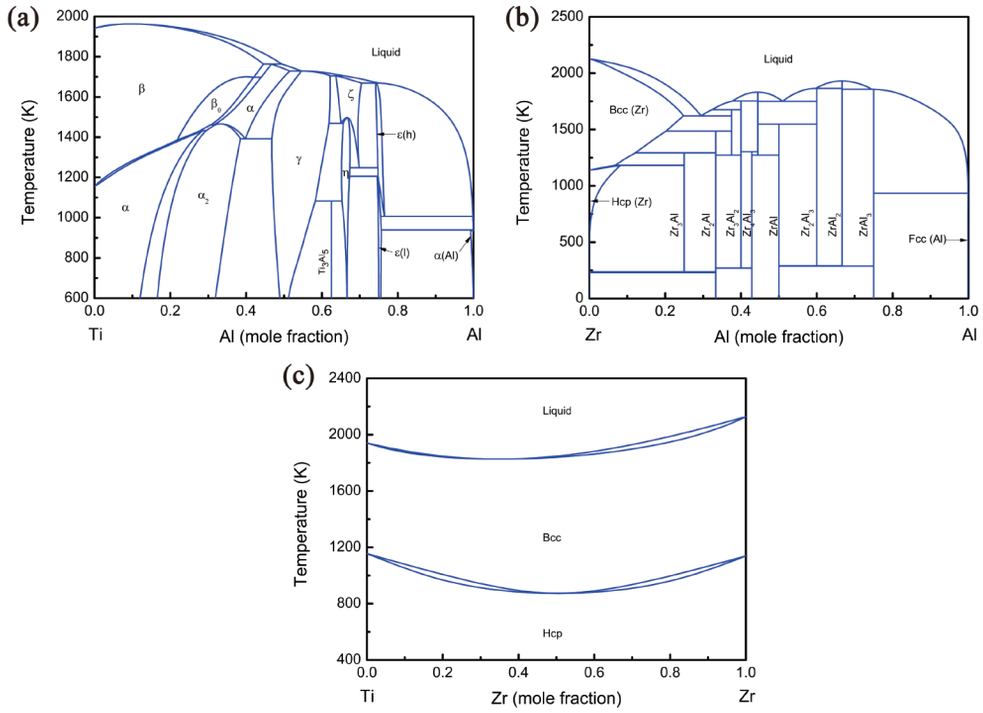

Figure 1. *The calculated phase diagram of (a) Ti–Al [28], (b) Al–Zr [36] and (c) Ti–Zr [48] binary systems*

Table 2. *Summary of the phase equilibria and thermodynamic data in the Ti–Al–Zr system*
DC = Diffusion couples; EA = Equilibrated alloys; EPMA = Electron probe microanalysis; XRD = X–ray diffraction; TEM = Transmission electron microscopy; MA = Microanalysis.; TA = Thermal Analysis

Reference	Type of data	Method
Shirokova et al. [49]	Vertical section of the Ti3Al to Ti+5%Zr(mass fraction)	EA, MA & TA
Kainuma et al. [50]	Partial isothermal sections at 1273, 1473 and 1573K in the Ti-rich corner	EA & EPMA
Premkumar et al. [54]	Phase relationships of aTi, bTi and g(TiAl) at 1473K	EA, XRD & TEM
Yang et al. [51]	Isothermal sections at 1273K	EA, XRD& EPMA
Lü et al. [52]	Isothermal sections at 1073K	DC, EA, & EPMA

as input data. The evaluation of the thermodynamic parameters was performed by the optimization program PARROT [60] of the Thermo-Calc software, which works by minimizing the square sum of the differences between measured and calculated values. Thermodynamic models used in the CALPHAD-type modeling are listed as follows.

3.2.1 Unary phases

The Gibbs energy function ${}^{\circ}G_i^{\varphi}(T) = G_i^{\varphi}(T) - H_i^{SER}$ for element i (i=Ti, Al, Zr) in the phase φ (φ=liquid, bcc_A2, hcp_A3 and fcc_A1) is expressed by the following equation:

$$ {}^{\circ}G_i^{\varphi}(T) = a + b\times T + c\times T\times \ln T + d\times T^2 + e\times T^{-1} + f\times T^3 + g\times T^7 + h\times T^{-9} \quad (2)$$

Where is the molar enthalpy of the element i at 298.15K and 1 bar in its standard element reference (SER) state, and T is the absolute temperature. In the present modeling, the Gibbs energies for pure elements (Ti, Al, Zr) were taken from the compilation by Dinsdale [61].

3.2.2 Solution phases

The Gibbs energies of solution phase j are expressed by the following equation:

$$ G_m^{\varphi} - H^{SER} = \sum_{i=1}^{n} x_i\, {}^{0}G_i^{\varphi} + RT\sum_{i=1}^{n} x_i \ln(x_i) + {}^{ex}G^{\varphi} \quad (3)$$

in which H^{SER} is the abbreviation of $x_{\mathrm{Ti}}\cdot H_{\mathrm{Ti}}^{\mathrm{SER}} + x_{\mathrm{Al}}\cdot H_{\mathrm{Al}}^{\mathrm{SER}} + x_{\mathrm{Zr}}\cdot H_{\mathrm{Zr}}^{\mathrm{SER}}$, x_i is the mole fractions of component

i (i=Ti, Al, Zr). ${}^{\circ}G_i^{\varphi}$ is the Gibbs energy for pure element i (i=Ti, Al, Zr) in the phase φ. R is the gas constant. ${}^{ex}G^{\varphi}$ is the excess Gibbs energy of the phase φ, which is described by Redlich–Kister polynomial [62]:

$$\begin{aligned} {}^{ex}G^{\varphi} &= x_{Ti}x_{Al}L^{\varphi}_{Ti,Al} + x_{Ti}x_{Zr}L^{\varphi}_{Ti,Zr} + \\ & x_{Al}x_{Zr}L^{\varphi}_{Al,Zr} + x_{Ti}x_{Al}x_{Zr}L^{\varphi}_{Ti,Al,Zr} \end{aligned} \quad (4)$$

$$L^{\varphi}_{i,j} = \sum_{m=0}^{n} {}^{m}L^{\varphi}_{i,j}(x_i - x_j)^m \quad (5)$$

$$L^{\varphi}_{Ti,Al,Zr} = x_{Ti}\,{}^{0}L^{\varphi}_{Ti,Al,Zr} + x_{Al}\,{}^{1}L^{\varphi}_{Ti,Al,Zr} + x_{Zr}\,{}^{2}L^{\varphi}_{Ti,Al,Zr} \quad (6)$$

Where $L^{\varphi}_{i,j}$ (i, j=Ti, Al, Zr, and $i \neq j$) are binary interaction parameters between i with j; ${}^{n}L^{\varphi}_{Ti,Al,Zr}$ is the ternary interaction parameter to be evaluated in the present work.

3.2.3 Intermetallic compounds

In the present work, the intermetallic compounds in the Ti–Al–Zr are divided into three types. The first type, such as the ZrAl and Zr_2Al_3 phases, is modeled as stoichiometric compounds. The Gibbs energy of each compound is given by the following expression:

$$\begin{aligned} {}^{\circ}G^{\mathrm{ZrxAly}}_{\mathrm{m}} - x_{Zr}H^{SER}_{Zr} - x_{Al}H^{SER}_{Al} &= \\ A + B\cdot T + x_{Zr}\,{}^{\circ}G^{hcp}_{Zr} + x_{Al}\,{}^{\circ}G^{fcc}_{Al} & \end{aligned} \quad (7)$$

in which A and B are to be evaluated.

The second type, i.e., $(Zr,Ti)_3Al$, $(Zr,Ti)_2Al$, $(Zr,Ti)_5Al_3$, $(Zr,Ti)_3Al_2$, $(Zr,Ti)_4Al_3$, $Zr(Al,Ti)_2$ and $(Zr,Ti)Al_3$, only one sublattice can be substituted. The Gibbs energy of these phases are given by the following expression:

$$\begin{aligned} {}^{\circ}G^{(\mathrm{Zr,Ti})x\mathrm{Al}y}_{\mathrm{m}} &= y'_{Zr}G^{\varphi}_{Zr:Al} + y'_{Ti}G^{\varphi}_{Ti:Al} + \\ & xRT(y'_{Ti}\ln y'_{Ti} + y'_{Zr}\ln y'_{Zr}) + y'_{Zr}y'_{Ti}\,{}^{\circ}L^{\varphi}_{Zr,Ti:Al} \end{aligned} \quad (8)$$

$$\begin{aligned} {}^{\circ}G^{\mathrm{Zrx(Al,Ti)}y}_{\mathrm{m}} &= y''_{Al}G^{\varphi}_{Zr:Al} + y''_{Ti}G^{\varphi}_{Zr:Ti} + \\ & yRT(y''_{Al}\ln y''_{Al} + y''_{Ti}\ln y''_{Ti}) + y''_{Al}y''_{Ti}\,{}^{\circ}L^{\varphi}_{Zr:Al,Ti} \end{aligned} \quad (9)$$

Where x, y denote the number of sites in each sublattice, y'_{Zr} and y'_{Ti} represent the site fractions of Zr and Al on the first sublattice, y''_{Al} and y''_{Ti} represent the site fractions of Al and Ti on the second sublattice. $G^{\varphi}_{Zr:Al}$, $G^{\varphi}_{Ti:Al}$, and $G^{\varphi}_{Zr:Ti}$ are the molar Gibbs energies of the end-members in the phase ${}^{\circ}L^{\varphi}_{Zr,Ti:Al}$, and ${}^{\circ}L^{\varphi}_{Zr:Al,Ti}$ represent interaction parameters between Zr and Al in the first sublattice and Al and Zr in the second sublattice, expressed by the Redlich-Kister polynomials.

The third type, in which two sublattices are substituted, is modelled as $(Ti, Al, Zr)_x$ (Ti, Al, $Zr)_y$, where the first sublattice is mainly occupied by Ti, the second by Al. x, y denote the number of sites in each sublattice. The Gibbs energy of the phase per mole-formula can be expressed as follows:

$$\begin{aligned} {}^{\circ}G^{\varphi}_{m} &= y'_{Ti}y''_{Ti}G^{\varphi}_{Ti:Ti} + y'_{Ti}y''_{Al}G^{\varphi}_{Ti:Al} + y'_{Ti}y''_{Zr}G^{\varphi}_{Ti:Zr} + \\ & y'_{Al}y''_{Ti}G^{\varphi}_{Al:Ti} + y'_{Al}y''_{Al}G^{\varphi}_{Al:Al} + y'_{Al}y''_{Zr}G^{\varphi}_{Al:Zr} \\ & + y'_{Zr}y''_{Ti}G^{\varphi}_{Zr:Ti} + y'_{Zr}y''_{Al}G^{\varphi}_{Zr:Al} + y'_{Zr}y''_{Zr}G^{\varphi}_{Zr:Zr} + \\ & xRT(y'_{Ti}\ln y'_{Ti} + y'_{Al}\ln y'_{Al} + y'_{Zr}\ln y'_{Zr}) \\ & + yRT(y''_{Ti}\ln y''_{Ti} + y''_{Al}\ln y''_{Al} + y''_{Zr}\ln y''_{Zr}) + \\ & y'_{Ti}y'_{Zr}y''_{Al}\,{}^{\circ}L^{\varphi}_{Ti,Zr:Al} + y'_{Ti}y''_{Al}y''_{Zr}\,{}^{\circ}L^{\varphi}_{Ti:Al,Zr} \\ & + y'_{Ti}y'_{Al}y''_{Al}\,{}^{\circ}L^{\varphi}_{Ti,Al:Al} + y'_{Ti}y'_{Al}y''_{Ti}\,{}^{\circ}L^{\varphi}_{Ti,Al:Ti} + \\ & y'_{Ti}y''_{Al}y''_{Ti}\,{}^{\circ}L^{\varphi}_{Ti:Al,Ti} + y'_{Al}y''_{Al}y''_{Ti}\,{}^{\circ}L^{\varphi}_{Al:Al,Ti} \end{aligned} \quad (10)$$

Where y'_{Ti}, y'_{Al} and y'_{Zr} represent the site fractions of Ti, Al and Zr on the first sublattice. y''_{Ti}, y''_{Al} and y''_{Zr} represent the site fractions of Ti, Al and Zr on the second sublattice. $G^{\varphi}_{Ti:Ti}$, $G^{\varphi}_{Ti:Al}$, $G^{\varphi}_{Ti:Zr}$, $G^{\varphi}_{Al:Ti}$, $G^{\varphi}_{Al:Al}$, $G^{\varphi}_{Al:Zr}$, $G^{\varphi}_{Zr:Ti}$, $G^{\varphi}_{Zr:Al}$ and $G^{\varphi}_{Zr:Zr}$ are the molar Gibbs energies of the end-members in the phase φ. The interaction between two species in one sublattice is assumed to be independent of the occupation of the other sublattice. ${}^{\circ}L^{\varphi}_{Ti,Zr:Al}$, ${}^{\circ}L^{\varphi}_{Ti:Al,Zr}$, ${}^{\circ}L^{\varphi}_{Ti,Al:Al}$, ${}^{\circ}L^{\varphi}_{Ti,Al:Ti}$, ${}^{\circ}L^{\varphi}_{Ti:Al,Ti}$ and ${}^{\circ}L^{\varphi}_{Al:Al,Ti}$ represent interaction parameters between different elements of the sublattice one and sublattice two.

4. Results and discussion

The experimental data of phase equilibria at 1073 K [52], 1273 K [51], the Ti-rich corner at 1273, 1473, and 1573 K [50], as well as a vertical section of the Ti_3Al–Ti + 5 wt.% Zr [49] were used to optimize this system. The parameters optimized in the present work were listed in table 3.

4.1 Lattice parameters and the formation enthalpies of the intermetallic compounds

The calculated lattice parameters of the intermetallic compounds of the Ti–Al and Al–Zr system are summarized and shown in Table 2 and Fig. 2. Fig. 2 (a) shows the lattice parameters of Ti–Al compounds that were calculated by *ab initio* along with literature data [24, 42, 43]. Fig. 2 (b) shows the Zr–Al compounds along with literature data [21, 29]. The calculated results fit very well with literature data, with a deviation of -0.35–1.46%.

The calculated formation enthalpies of the intermetallic compounds of the Ti–Al and Al–Zr system are summarized and shown in Table 4 and Fig. 3. Fig. 3 (a) shows the formation enthalpies of Ti–Al system with reference data [63-66], showing a good agreement. Fig. 3 (b) presents the comparison between the formation enthalpies of Zr–Al system and the data available in the literature [33, 34, 36, 38, 67, 68]. The calculated results have a good agreement with literature data except Wang et al. [36]. The results from Wang et al. [36] are obtained by calculation, and the results of other researchers are gained through experiments. Therefore, our results are reliable.

Table 3. *Summary of the thermodynamic parameters in the Ti–Al–Zr system by the present work.DC = Diffusion couples; EA = Equilibrated alloys; EPMA = Electron probe microanalysis; XRD = X–ray diffraction; TEM = Transmission electron microscopy; MA = Microanalysis.; TA = Thermal Analysis*

Phase	Models	Parametes
Liquid	(Al, Ti, Zr)$_1$	${}^0L^{Liquid}_{Al,Ti,Zr} = -200000$
HCP_A3	(Al, Ti, Zr)$_1$Va$_{0.5}$	${}^0L^{HCP\_A3}_{Al,Ti,Zr:Va} = -32190 - 30T$
		${}^1L^{HCP\_A3}_{Al,Ti,Zr:Va} = 107300 - 100T$
BCC_A2	(Al, Ti, Zr)$_1$Va$_3$	${}^0L^{BCC\_A2}_{Al,Ti,Zr:Va} = -100000$
		${}^2L^{BCC\_A2}_{Al,Ti,Zr:Va} = -50000$
BCC_B2	(Al, Ti, Zr)$_{0.5}$(Al, Ti, Zr)$_{0.5}$Va	${}^0L^{BCC\_B2}_{Al,Ti:Zr:Va} = -20000$
		${}^0G^{Ti_3Al}_{Zr:Al} = +{}^\circ G^{FCC}_{Al} + 3\,{}^\circ G^{HCP}_{Zr} - 110656$
Ti_3Al	(Ti, Al, Zr)$_3$(Ti, Al, Zr)$_1$	${}^0L^{Liquid}_{Al,Ti,Zr} = -200000$
		${}^0G^{Ti_3Al}_{Zr:Al} = +{}^\circ G^{FCC}_{Al} + 3\,{}^\circ G^{HCP}_{Zr} - 110656$
		${}^0G^{Ti_3Al}_{Ti:Zr} = +3\,{}^\circ G^{HCP}_{Ti} + {}^\circ G^{HCP}_{Zr} + 12632 + 8T$
		${}^0G^{Ti_3Al}_{Zr:Zr} = +4\,{}^\circ G^{HCP}_{Zr} + 316$
		${}^0G^{Ti_3Al}_{Al:Zr} = 3\,{}^\circ G^{FCC}_{Al} + {}^\circ G^{HCP}_{Zr}$
		${}^0G^{Ti_3Al}_{Zr:Ti} = +3\,{}^\circ G^{HCP}_{Zr} + {}^\circ G^{HCP}_{Ti} + 13000$
		${}^0L^{Ti_3Al}_{Ti,Zr:Al} = +19000 - 40T$
TiAl	(Ti, Al, Zr)$_1$(Ti, Al, Zr)$_1$	${}^0L^{Ti_3Al}_{Al,Ti,Zr:Al} = -400000$
		${}^0G^{TiAl}_{Al:Zr} = +{}^\circ G^{HCP}_{Zr} + {}^\circ G^{FCC}_{Al} - 83980 + 8T$
		${}^0G^{TiAl}_{Zr:Ti} = +{}^\circ G^{HCP}_{Ti} + {}^\circ G^{HCP}_{Zr} + 18160$
		${}^0G^{TiAl}_{Zr:Zr} = +2\,{}^\circ G^{HCP}_{Zr} + 7560$
		${}^0G^{TiAl}_{Zr:Al} = +{}^\circ G^{FCC}_{Al} + {}^\circ G^{HCP}_{Zr}$
		${}^0G^{TiAl}_{Ti:Zr} = +{}^\circ G^{HCP}_{Zr} + {}^\circ G^{HCP}_{Ti}$
		${}^0L^{TiAl}_{Al:Ti,Zr} = -24000$
		${}^0L^{TiAl}_{Al,Zr:Ti} = -100000$
$TiAl_2$	(Ti, Al, Zr)$_2$(Ti, Al, Zr)$_1$	${}^0L^{TiAl}_{Al:Ti,Al,Zr} = -200000$
		${}^0G^{TiAl_2}_{Al:Zr} = +{}^\circ G^{HCP}_{Zr} + 2\,{}^\circ G^{FCC}_{Al} - 136690 + 5T$
		${}^0G^{TiAl_2}_{Zr:Ti} = +{}^\circ G^{HCP}_{Ti} + 2\,{}^\circ G^{HCP}_{Zr} + 23880$
		${}^0G^{TiAl_2}_{Zr:Zr} = +3\,{}^\circ G^{HCP}_{Zr} + 11400$
		${}^0G^{TiAl_2}_{Zr:Al} = +{}^\circ G^{FCC}_{Al} + 2\,{}^\circ G^{HCP}_{Zr}$
		${}^0G^{TiAl_2}_{Ti:Zr} = +{}^\circ G^{HCP}_{Zr} + 2\,{}^\circ G^{HCP}_{Ti}$
$TiAl_3$ (h)	(Ti, Al, Zr)$_3$(Ti, Al, Zr)$_1$	${}^0G^{TiAl_2}_{Al:Ti,Zr} = -30000$
		${}^0G^{TiAl_3(h)}_{Al:Zr} = +{}^\circ G^{HCP}_{Zr} + 3\,{}^\circ G^{FCC}_{Al} - 167403 + 10T$
		${}^0G^{TiAl_3(h)}_{Zr:Ti} = +{}^\circ G^{HCP}_{Ti} + 3\,{}^\circ G^{HCP}_{Zr} + 35896$
		${}^0G^{TiAl_3(h)}_{Zr:Zr} = +4\,{}^\circ G^{HCP}_{Zr} + 446764$
		${}^0G^{TiAl_3(h)}_{Zr:Al} = +{}^\circ G^{FCC}_{Al} + 3\,{}^\circ G^{HCP}_{Zr}$
		${}^0G^{TiAl_3(h)}_{Ti:Zr} = +{}^\circ G^{HCP}_{Zr} + 3\,{}^\circ G^{HCP}_{Ti}$
		${}^0L^{Zr_3Al}_{Al:Zr,Ti} = -72000$

***table continues on the next line**

***table continued from the previous line**

$TiAl_3$ (l)	(Ti, Al, Zr)$_3$(Ti, Al, Zr)$_1$	${}^0G^{TiAl_3(l)}_{Al:Zr} = +{}^\circ G^{HCP}_{Zr} + 3\,{}^\circ G^{FCC}_{Al} - 178860 + 20T$
		${}^0G^{TiAl_3(l)}_{Zr:Ti} = +{}^\circ G^{HCP}_{Ti} + 3\,{}^\circ G^{HCP}_{Zr} + 35896$
		${}^0G^{TiAl_3(l)}_{Zr:Zr} = +4\,{}^\circ G^{HCP}_{Zr} + 446764$
		${}^0G^{TiAl_3(l)}_{Zr:Al} = +{}^\circ G^{FCC}_{Al} + 3\,{}^\circ G^{HCP}_{Zr}$
		${}^0G^{TiAl_3(l)}_{Ti:Zr} = +{}^\circ G^{HCP}_{Zr} + 3\,{}^\circ G^{HCP}_{Ti}$
Ti_2Al_5	(Ti, Al, Zr)$_5$(Ti, Al, Zr)$_2$	${}^0G^{Ti_2Al_5}_{Al:Zr} = +2\,{}^\circ G^{HCP}_{Zr} + 5\,{}^\circ G^{FCC}_{Al} - 310450 + 14T$
		${}^0G^{Ti_2Al_5}_{Zr:Ti} = +2\,{}^\circ G^{HCP}_{Ti} + 5\,{}^\circ G^{HCP}_{Zr} + 80000$
		${}^0G^{Ti_2Al_5}_{Zr:Zr} = +7\,{}^\circ G^{HCP}_{Zr} + 80000$
		${}^0G^{Ti_2Al_5}_{Zr:Al} = +2\,{}^\circ G^{FCC}_{Al} + 5\,{}^\circ G^{HCP}_{Zr}$
		${}^0G^{Ti_2Al_5}_{Ti:Zr} = +2\,{}^\circ G^{HCP}_{Zr} + 5\,{}^\circ G^{HCP}_{Ti}$
		${}^0G^{Ti_2Al_5}_{Al:Ti,Zr} = -11000 - 30T$
Zr_3Al	Al_1(Zr, Al)$_3$	${}^0G^{Zr_3Al}_{Al:Ti} = +{}^\circ G^{FCC}_{Al} + 3\,{}^\circ G^{HCP}_{Ti} - 40000$
		${}^0L^{Zr_3Al}_{Al:Zr,Ti} = -72000$
Zr_2Al	(Al)$_1$(Zr, Ti)$_2$	${}^0G^{Zr_2Al}_{Al:Ti} = +{}^\circ G^{FCC}_{Al} + 2\,{}^\circ G^{HCP}_{Ti} - 74160 + 15T$
		${}^0L^{Zr_2Al}_{Al:Zr,Ti} = +70500 - 90T$
Zr_5Al_3	Al_3(Zr, Ti)$_5$	${}^0G^{Zr_5Al_3}_{Al:Ti} = +3\,{}^\circ G^{FCC}_{Al} + 5\,{}^\circ G^{HCP}_{Ti} - 201120 + 40T$
		${}^0L^{Zr_5Al_3}_{Al:Zr,Ti} = 89600 - 160T$
Zr_3Al_2	Al_2(Zr, Ti)$_3$	${}^0G^{Zr_3Al_2}_{Al:Ti} = +2\,{}^\circ G^{FCC}_{Al} + 3\,{}^\circ G^{HCP}_{Ti} - 100000 + 25T$
		${}^0L^{Zr_3Al_2}_{Al:Zr,Ti} = -272775 + 175T$
Zr_4Al_3	(Al)$_3$(Zr, Ti)$_4$	${}^0G^{Zr_4Al_3}_{Al:Ti} = +3\,{}^\circ G^{FCC}_{Al} + 4\,{}^\circ G^{HCP}_{Ti} - 232281 + 70T$
		${}^0L^{Zr_4Al_3}_{Al:Zr,Ti} = -168210 + 70T$
$ZrAl_2$	(Al, Ti)$_2$(Zr)$_1$	${}^0G^{ZrAl_2}_{Ti:Zr} = +2\,{}^\circ G^{HCP}_{Ti} + 1\,{}^\circ G^{HCP}_{Zr} + 50133$
		${}^0L^{ZrAl_2}_{Al,Ti:Zr} = -296760 + 129T$
$ZrAl_3$	Al_3(Zr, Ti)$_1$	${}^0G^{ZrAl_3}_{Al:Ti} = +3\,{}^\circ G^{FCC}_{Al} + {}^\circ G^{HCP}_{Ti} - 128724 + 25.8T$
		${}^0L^{ZrAl_3}_{Al:Zr,Ti} = -25460 + 20T$

4.2 Vertical section

Fig. 4 shows the calculated vertical section of the Ti_3Al–Ti + 5 wt.% Zr by PANDAT [69] software, and the experimental data from Shirokova et al. [49]. It can be seen that the calculation results are in good agreement with the experimental values.

4.3 Isothermal section

Fig. 5 (a)–(c) shows the calculated isothermal sections of the Ti-rich corner of the Ti–Al–Zr system at 1273, 1473, and 1573 K, respectively. The experimental points [50] are marked as a black circle. At 1273 and 1473 K, compared to the experimental data, the optimization results are not very good. Especially for a(hcp_A3) phase, not all the experimental points are on the phase boundary. When the a(hcp_A3) phase parameters of the Ti–Al binary system [28] are adjusted, this can be avoided. It may

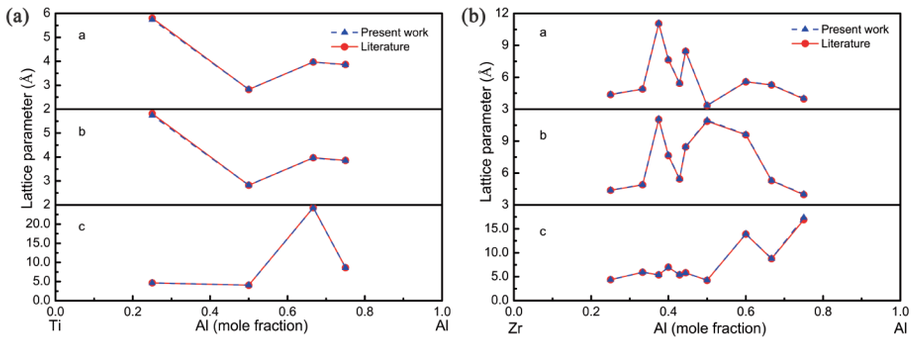

Figure 2. *Variation of lattice parameters of (a) Ti–Al binary system along with references [24, 42, 43] and (b) Zr–Al binary system along with references [21, 29]*

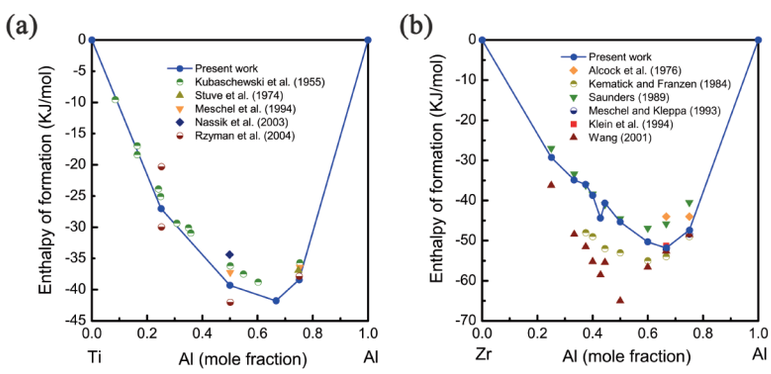

Figure 3. *The enthalpy of formation of (a) Ti–Al binary system (reference state is hcp Ti and fcc Al) along with the experimental data [63-66] and (b) Zr–Al binary system (reference state is hcp Zr and fcc Al) along with the experimental data [33, 34, 36, 38, 67, 68]*

Table 4. *Summary of formation enthalpies of the Ti-Al intermetallic compounds, kJ/(mole of atoms)*

Compounds	Kubaschewski [63]	Stuve [64]	Meschel [65]	Nassik [66]	This work (cal.)
Ti_3Al	–	–	–	–	-27.01
TiAl	-40.1	–	–	-35.1	-39.3
$TiAl_2$	-40.9	–	–	-37.1	-41.79
$TiAl_3$	-36.6	-36.9	-36.6	-47	-38.39

Table 5. *Summary of formation enthalpies of the Zr-Al intermetallic compounds, kJ/(mole of atoms)*

Compounds	Kematick [38]	Alcock [67]	Meschel [34]	Klein [33]	Saunders [68]	Wang [36]	This work (cal.)
Zr_3Al	–	–	–	–	-27	-36.2	-29.2
Zr_2Al	–	–	–	–	-33.4	-48.4	-34.9
Zr_5Al_3	-48	–	–	–	-36.2	-51.5	-36
Zr_3Al_2	-49	–	–	–	-38.4	-55.2	-38.7
Zr_4Al_3	–	–	–	–	–	-58.5	-44.4
Zr_5Al_4	-52	–	–	–	-41	-55.4	-40.6
ZrAl	-53	–	–	–	-44.5	-65	-45.3
Zr_2Al_3	-55	–	–	–	-46.9	-56.6	-50.4
$ZrAl_2$	-54	-44	-52.1	-51.3	-45.8	-52.6	-51.8
$ZrAl_3$	-49	-44	-48.4	–	-40.5	-48.5	-47.4

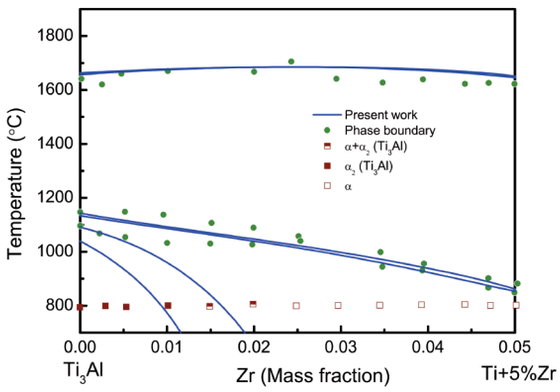

Figure 4. *Selected isopleth in the Ti–Al–Zr system showing calculated equilibria (lines). Experimental data [49] are shown as symbols*

result from the error of the parameters [28] at the a(hcp_A3) phase in Ti-Al binary system. Generally, the phase relationships are correct, and the optimization results are acceptable. At 1573 K, the $a_2(Ti_3Al)$ phase and the g(TiAl) phase are in good agreement with the experimental data.

Fig. 6 (a) is the calculated isothermal section of the Ti–Al–Zr system at 1073 K. There are 15 three-phase regions inside. Eight of them have been proved to exist by Lü et al [52]. Six of them are concluded by experiments. The remaining one phase appears in the present work. For the eight three-phase regions which have been proved to exist by experiment [52]. $e(TiAl_3\ h) + \eta(TiAl_2) + ZrAl_3$, $\eta(TiAl_2) + ZrAl_3 + ZrAl_2$, $\eta(TiAl_2) + ZrAl_2 + g(TiAl)$, $ZrAl_2 + Zr_2Al_3 + Zr_4Al_3$ and $Zr_3Al_2 + Zr_2Al + b(Ti, Zr)$ are obtained by equilibrated alloys. But the $ZrAl_2 + Zr_2Al_3 + Zr_4Al_3$ and $Zr_3Al_2 + Zr_2Al + b(Ti, Zr)$ are not in good agreement with experimental points. Considering the measuring error in experiments, this small difference between the calculated phase diagram and the experimental data can be acceptable. Other three three-phase regions fit well with experimental data. $a(Ti) + a_2(Ti_3Al) + b(Ti, Zr)$, $a_2(Ti_3Al) + b(Ti, Zr) + g(TiAl)$ and $b(Ti, Zr) + g(TiAl) + ZrAl_2$ three-phase regions are gained by diffusion couple. Two three-phase regions of $TiAl + Ti_3Al + b(Ti, Zr)$ and $TiAl + ZrAl_2 + b(Ti, Zr)$ were proposed by Lü et al [52], while our calculations show phase equilibria of $TiAl + Ti_3Al + Zr_4Al_3$ and $TiAl + ZrAl_2 + Zr_4Al_3$ at 1073 K. However, direct experimental proof of the two three-phase regions is not presented in Lü et al. [52], and further experiments are needed. It is also found that introduction of ternary parameters cannot alter the phase relationship to fit the results in Lü et al. [52]. Adjusting the binary parameters can be carried out but only based on future solid experimental evidence. The other six three-phase regions, $liquid + e(TiAl_3\ h) + ZrAl_3$, $Zr_2Al_3 + Zr_4Al_3 + ZrAl$, $Zr_4Al_3 + a_2(Ti_3Al) + b(Ti, Zr)$, $Zr_4Al_3 + Zr_3Al_2 + b(Ti, Zr)$, $Zr_2Al + Zr_3Al + b(Ti, Zr)$ and $Zr_3Al + b(Ti, Zr) + a(Zr)$, are reasonably inferred by the experiment. It appears in the present work. But one of them is different from the experiments. $a_2(Ti_3Al) + Zr_4Al_3 + b(Ti, Zr)$, appears in the optimized isothermal section while $ZrAl_2 + Zr_4Al_3 + b(Ti, Zr)$ appears in the experimental phase diagram. There is one new three-phase region in this isothermal section compared with the experimental data, and the region is $e(TiAl_3\ h) + e(TiAl_3\ l) + TiAl_2$. In the binary phase diagram of Ti–Al at 1073 K [28], the $e(TiAl_3)$ existed both at high and low temperature, so the existence of this region is reasonable. Over the whole composition range, the result is acceptable.

Fig. 6 (b) is the calculated isothermal section of the Ti–Al–Zr system at 1273 K. This isothermal section includes 14 three-phase regions. Among them, ten three-phase regions have been completely determined by Yang et al. [51]. $e(TiAl_3\ h) + \zeta(Ti_2Al_5) + ZrAl_3$, $\zeta(Ti_2Al_5) + ZrAl_3 + \eta(TiAl_2)$, $ZrAl_3 + ZrAl_2 + \eta(TiAl_2)$, $\eta(TiAl_2) + ZrAl_2 + g(TiAl)$, $g(TiAl) + ZrAl_2 + Zr_5Al_3$, $ZrAl_2 + Zr_2Al_3 + Zr_5Al_3$, $Zr_2Al_3 + Zr_4Al_3 + Zr_5Al_3$, $g(TiAl) + Zr_5Al_3 + a_2(Ti_3Al)$, $a_2(Ti_3Al) + a(Zr) + b(Ti, Zr)$ and $Zr_5Al_3 + Zr_2Al + b(Ti, Zr)$, which are represented by red areas. Nine three-phase regions are in good agreement with experimental points, except $Zr_2Al_3 + Zr_4Al_3 + Zr_5Al_3$. The alloy composition prepared by Yang et al. [51] is out of the $Zr_2Al_3 + Zr_4Al_3 + Zr_5Al_3$ three-phase region. It was found that the phase equilibrium is strongly affected by the negative Gibbs energy of the ZrAl phase at 1273 K, one can only adjust the thermodynamic parameters of this phase to fit the experimental data. However, it is beyond the scope of the present work to modify the binary system based on one single ternary experimental point. Therefore, instead of the alloy composition data, only the phase relationship $Zr_2Al_3 + Zr_4Al_3 + Zr_5Al_3$ was considered in the optimization. The remaining four three-phase regions, $liquid + e(TiAl_3\ h) + ZrAl_3$, $Zr_2Al_3 + Zr_4Al_3 + ZrAl$, $Zr_4Al_3 + Zr_3Al_2 + Zr_5Al_3$ and $b(Ti, Zr) + a_2(Ti_3Al) + Zr_5Al_3$, are reasonably inferred by experiment, which are represented by green areas in the figure.

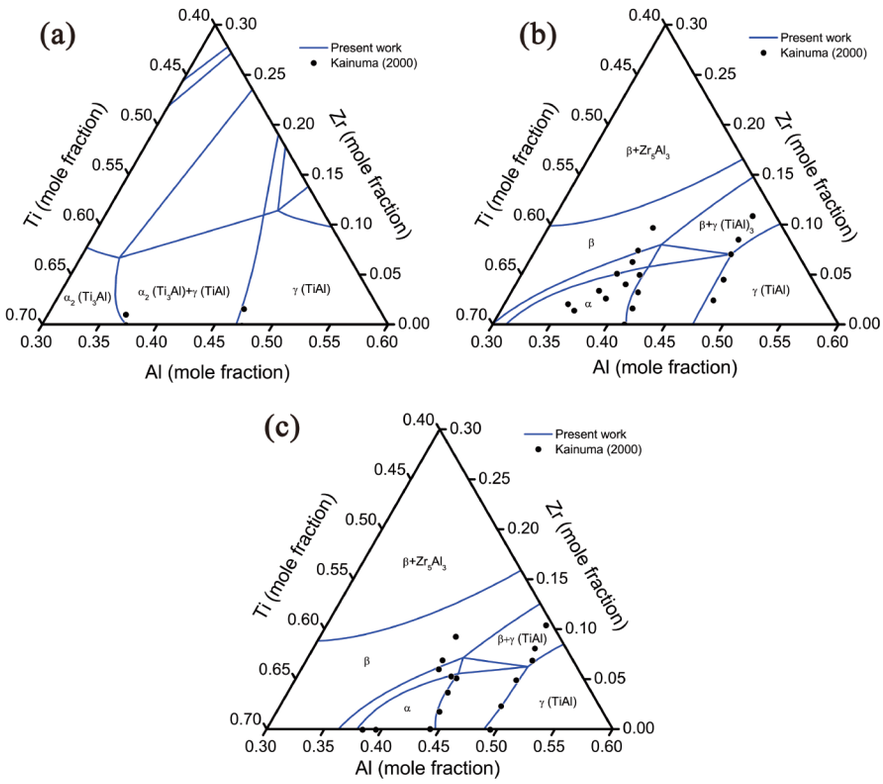

Figure 5. *Phase boundary of the Ti-rich corner of the Ti–Al–Zr ternary system at (a) 1273 K, (b) 1473 K and (c) 1573 K, along with experimental data [50]*

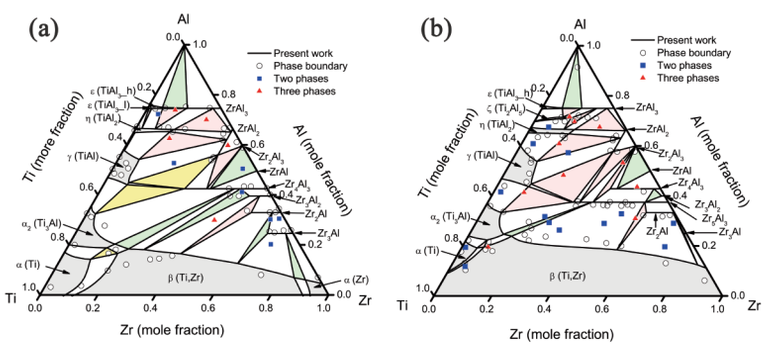

Figure 6. *Calculated isothermal section of Ti–Al–Zr system at (a)1073 K, compared with the experimental data [51] and (b) 1273 K, compared with the experimental data [52]*

5. Conclusions

The Ti–Al–Zr system has been thermodynamically investigated with the three sub-binary systems and ternary experimental phase diagram data using *ab initio* calculations and the CALPHAD method. The Ti–Al–Zr ternary dataset is established. The results can be summarized as follows:

1. The lattice parameters and the total energy of related phases are calculated by *ab initio*, and the results are in good accordance with the experimental data.

2. The calculated isothermal section of the Ti–Al–Zr system at 1273 K is in close agreement with the experimental data. For the isothermal section at 1073 K, the three-phase regions of TiAl + Ti_3Al + b(Ti, Zr) and TiAl + $ZrAl_2$ + b(Ti, Zr) cannot be reproduced and more experimental data are needed. The results of the

Ti-rich corner of the Ti–Al–Zr system at 1273, 1473, and 1573 K are consistent with the experimental values as well. The Ti_3Al–Ti + 5 wt.% Zr vertical section of the Ti–Al–Zr system is in good agreement with experiments.

3. One new three-phase region at 1073 K has been predicted by the calculation, i.e., e($TiAl_3$ h) + e($TiAl_3$ l) + $TiAl_2$. The existence of this region is reasonable through our analysis compared with the experimental data.

Acknowledgement

Financial support from National Natural Science Foundation of China (51604104 and 51701232) and CAS Pioneer Hundred Talents Program is acknowledged.

References

[1] E. Bayraktar, Int. J. Fatigue, 26 (2004) 1263-1275.
[2] T.G. Nieh, L.M. Hsiung, J. Wadsworth, Intermetallics, 7 (1997) 163-170.
[3] Y. Wang, Y. Liu, G. Yang, H. Li, B. Tang, Trans. Nonferrous Met. Soc. China, 21 (2011) 215-222.
[4] W. Chen, Y. Guan, Z. Wang, Trans. Nonferrous Met. Soc. China, 26 (2016) 369-377.
[5] C.T. Liu, J.L. Wright, S.C. Deevi, Mater. Sci. Eng., A, 329-331 (2002) 416-423.
[6] Y. Jin, J.N. Wang, J. Yang, Y. Wang, Scr. Mater., 51 (2004) 113-117.
[7] G. Hénaff, A.-L. Gloanec, Intermetallics, 13 (2005) 543-558.
[8] A. Luo, M. Pekguleryuz, J. Mater. Sci., 29 (1994) 5259-5271.
[9] Y. Ke, H. Duan, Y. Sun, Mater. Sci. Eng., A, 528 (2010) 220-225.
[10] G.S. Fox-Rabinovich, D.S. Wilkinson, S.C. Veldhuis, G.K. Dosbaeva, G.C. Weatherly, Intermetallics, 14 (2006) 189-197.
[11] C.Z. Qiu, Y. Liu, L. Huang, W. Zhang, B. Liu, B. Lu, Trans. Nonferrous Met. Soc. China, 22 (2012) 521-527.
[12] K. Hashimoto, H. Doi, K. Kasahara, T. Tsujimoto, T. Suzuki, J. Jpn. Inst. Met., 52 (1988) 816-825.
[13] X.J. Jiang, Y.K. Zhou, Z.H. Feng, C.Q. Xia, C.L. Tan, S.X. Liang, X.Y. Zhang, M.Z. Ma, R.P. Liu, Mater. Sci. Eng., A, 639 (2015) 407-411.
[14] N.A. Belov, A.N. Alabin, I.A. Matveeva, D.G. Eskin, Trans. Nonferrous Met. Soc. China, 25 (2015) 2817-2826.
[15] G.J. Fan, X.P. Song, M.X. Quan, Z.Q. Hu, Mater. Sci. Eng., A, 231 (1997) 111-116.
[16] F. Wang, D. Qiu, Z.L. Liu, J. Taylor, M. Easton, M.X. Zhang, Trans. Nonferrous Met. Soc. China, 24 (2014) 2034-2040.
[17] X.J. Liu, H. Luo, Y. Lu, J.J. Han, J. Li, Y.H. Guo, Y.X. Huang, C.P. Wang, J. Phase Equilib. Diffus., 38 (2017) 897-905.
[18] K. Chang, B. Hallstedt, D. Music, Chem. Mater., 24 (2012) 97–105.
[19] K. Chang, S. Liu, D. Zhao, Y. Du, L. Zhou, L. Chen, Thermochim. Acta, 512 (2011) 258-267.
[20] A. Grytsiv, P. Rogl, H. Schmidt, G. Giester, J. Phase Equilib., 24 (2003) 511-527.
[21] R. Schmid-Fetzer, MSIT Binary Evaluation Program, in MSIT Workplace, Effenberg, G., MSI, Materials Science International Services, GmbH, Stuttgart, (2003).
[22] J. Braun, PhD Thesis, Max-Planck-Institut für Metallforschumg, Stuttgart, 1999, pp. 1–283 (in German).
[23] J. Braun, M. Ellner, Z. Metallkd., 91 (2000) 389-392 (in German).
[24] J. Braun, M. Ellner, Metall. Mater. Trans. A, 32 (2001) 1037-1047.
[25] F. Zhang, S.L. Chen, Y.A. Chang, U.R. Kattner, Intermetallics, 5 (1997) 471-482.
[26] I. Ansara, A.T. Dinsdale, M.H. Rand, COST 507, 2 (1998).
[27] I. Ohnuma, Y. Fujita, H. Mitsui, K. Ishikawa, R. Kainuma, K. Ishida, Acta Mater., 48 (2000) 3113-3123.
[28] V.T. Witusiewicz, A.A. Bondar, U. Hecht, S. Rex, T.Y. Velikanova, J. Alloys Compd., 465 (2008) 64-77.
[29] J. Murray, A. Peruzzi, J. Abriata, J. Phase Equilib., 13 (1992) 277-291.
[30] H. Okamoto, J. Phase Equilib., 14 (1993) 259-260.
[31] A. Peruzzi, J. Nucl. Mater., 186 (1992) 89-99.
[32] G. Batalin, E. Beloborodova, V. Nerubaschenko, V. Galochka, L. Slyuzko, Izv. Vyssh. Ucheb. Zaved. Tsvetn. Metall, 3 (1982) 74-77.
[33] R. Klein, I. Jacob, P. O'Hare, R. Goldberg, J. Chem. Thermodyn., 26 (1994) 599-608.
[34] S.V. Meschel, O.J. Kleppa, J. Alloys Compd., 191 (1993) 111-116.
[35] Y.O. Esin, N. Serebrennikov, E. Pletneva, V. Kapustkin, Izv. Vyssh. Uchebn. Zaved., Chern. Metall., (1987) 1-3.
[36] T. Wang, Z. Jin, J.-C. Zhao, J. Phase Equilib., 22 (2001) 544-551.
[37] S.N. Tiwari, K. Tangri, J. Nucl. Mater., 32 (1970) 92-96.
[38] R. Kematick, H. Franzen, J. Solid State Chem., 54 (1984) 226-234.
[39] P. Malek, M. JaneČek, B. Smola, P. BartuŠka, J. PleŠtil, J. Mater. Sci., 35 (2000) 2625-2633.
[40] H.W. King, J. Phase Equilib., 2 (1981) 402.
[41] T.B. Massalski, J. Murray, L. Bennett, H. Baker, American Society for Metals, (1986) 2224.
[42] J. Schuster, J. MSIT Bin. Eval. Progr, (2003).
[43] M. Karpets, Y.V. Milman, O. Barabash, N. Korzhova, O. Senkov, D. Miracle, T. Legkaya, I. Voskoboynik, Intermetallics, 11 (2003) 241-249.
[44] J. Murray, Bull. Alloy Phase Diagrams, 2 (1981) 197-201.
[45] J. Murray, ASM international, (1987) 340-345.
[46] V. Kuprina, V. Bernard, A. Grigor'ev, E. Sokolovskaya, Vestn. Moskov. Univ., Ser. II, Khim., No. 5, 69-73 . (1966).
[47] J. Blacktop, J. Crangle, B. Argent, J. Less-Common Met., 109 (1985) 375-380.
[48] K.C. Hari Kumar, P. Wollants, L. Delaey, J. Alloys

Compd., 206 (1994) 121-127.
[49] N.I. Shirokova, T.T. Nartova, I.I. Kornilov, Izv. Akad. Nauk SSR Met., 13 (1968) 183-193.
[50] R. Kainuma, Y. Fujita, H. Mitsui, I. Ohnuma, K. Ishida, Intermetallics, 8 (2000) 855-867.
[51] F. Yang, F.H. Xiao, S.G. Liu, S.S. Dong, L.H. Huang, Q. Chen, G.M. Cai, H.S. Liu, Z.P. Jin, J. Alloys Compd., 585 (2014) 325-330.
[52] K.-l. LÜ, F. Yang, Z.-y. Xie, H.-s. Liu, G.-m. Cai, Z.-p. Jin, Trans. Nonferrous Met. Soc. China, 26 (2016) 3052-3058.
[53] G. Ghosh, S. Vaynman, M. Asta, M.E. Fine, Intermetallics, 15 (2007) 44-54.
[54] M. Premkumar, K.S. Prasad, A.K. Singh, Intermetallics, 17 (2009) 142-145.
[55] G. Kresse, J. Furthmüller, Phys. Rev. B, 54 (1996) 11169.
[56] G. Kresse, D. Joubert, Phys. Rev. B, 59 (1999) 1758.
[57] P.E. Blöchl, Phys. Rev. B, 50 (1994) 17953.
[58] H.J. Monkhorst, J.D. Pack, Phys. Rev. B, 13 (1976) 5188-5192.
[59] Y. Du, R. Schmid-Fetzer, H. Ohtani, Z. Metallkd., 88 (1997) 545-556.
[60] B. Sundman, B. Jansson, J.-O. Andersson, Calphad, 9 (1985) 153-190.
[61] A.T. Dinsdale, Calphad, 15 (1991) 317-425.
[62] O. Redlich, A. Kister, Ind. Eng. Chem., 40 (1948) 341-345.
[63] O. Kubaschewski, W.A. Dench, Acta Metall., 3 (1955) 339-346.
[64] J.M. Stuve, M.J. Ferrante, US Bur. Mines, Rep. Invest. #7834, Washington, DC, (1974) pp. 1-9.
[65] S. Meschel, O. Kleppa, J. Faulkner, R. Jordan, NATO ASI Ser., Ser. E, 256 (1994) 103.
[66] M. Nassik, F. Chrifi-Alaoui, K. Mahdouk, J. Gachon, J. Alloys Compd., 350 (2003) 151-154.
[67] C. Alcock, S. Zador, K. Jacob, (1976).
[68] N. Saunders, Z. Metallkd., 80 (1989) 894-903.
[69] PANDAT Software, version 8.1, CompuTherm LLC, Madison, WI.

AB INITIO I CALPHAD TERMODINAMIČKO ISPITIVANJE Ti–Al–Zr SISTEMA

Z.-X. Deng [a,b], D.-P. Zhao [a,*], Y.-Y. Huang [b], L.-L. Chen [b], H. Zou [b], Y. Jiang [b], K. Chang [b,*]

[a*]Biološki fakultet, Univerzitet u Hjunanu, Čangša, Hjunan, Kina
[b] Inženjerska laboratorija materijala nuklearne energije, Ningbo institut za tehnologiju i inženjerstvo materijala, Kineska akademija nauka, Zeidžang, Kina

Apstrakt

Legure na bazi Ti–Al imaju široku primenu u aeronautici i svemirskoj industriji. Dodavanjem Zr kao legirajućeg elementa može značajno da se poboljša otpornost na visoku temperaturu i koroziju. Da bi se ispitao uticaj koji dodavanje Zr ima na osobine Ti–Al sistema, korišćeni su metodi ab initio proračuna i CALPHAD (proračun faznog dijagrama) da bi se odredio Ti-Al–Zr trojni system. Ab initio proračun je izvršen da bi se izračunale entalpije formiranja intermetalnih jedinjenja i krajnjih članova. CALPHAD pristup je primenjen da bi se optimizirali termodinamički parametri zasnovani na eksperimentima. Eksperimentalni podaci fazne ravnoteže pri temperaturama od 1073, 1273, 1473, i 1573 K, kao i vertikalni presek Ti3Al–Ti + 5 wt.% Zr su korišćeni da bi se ovaj sistem termodinamički optimizovao. Termodinamički parametri binarnih Ti–Al, Al–Zr i Ti–Zr sistema dobijeni su iz nedavno izvršenih optimizacija, a trojni parametri su procenjeni u ovom radu. Utvrđen je set podataka za trojni sistem Ti–Al–Zr, i rezultati proračuna su u skladu sa eksperimentalnim podacima koji se tiču i termodinamičke i fazne ravnoteže.

***Ključne reči**: Ti–Al–Zr sistem; Ab initio proračun; Fazni dijagrami; Termodinamička optimizacija*